

ORIGINAL PAPER

Boundary operation of 2D non-separable oversampled lapped transforms

KOSUKE FURUYA¹, SHINTARO HARA², KENTA SEINO¹ AND SHOGO MURAMATSU³

This paper proposes a boundary operation technique of two-dimensional (2D) non-separable oversampled lapped transforms (NSOLT). The proposed technique is based on a lattice structure consisting of the 2D separable block discrete cosine transform and non-separable redundant support-extension processes. The atoms are allowed to be anisotropic with the oversampled, symmetric, real-valued, compact-supported, and overlapped property. First, the blockwise implementation is developed so that the atoms can be locally controlled. The local control of atoms is shown to maintain perfect reconstruction. This property leads an atom termination (AT) technique as a boundary operation. The technique overcomes the drawback of NSOLT that the popular symmetric extension method is invalid. Through some experimental results with iterative hard thresholding, the significance of AT is verified.

Keywords: Non-separable oversampled lapped transforms (NSOLTs), Multidimensional filter banks, Size-limitation, Iterative hard thresholding

Received 3 March 2015; Accepted 8 February 2016

1. INTRODUCTION

Filter banks and transforms are essential components of signal processing and there are a wide variety of applications such as compression, communication, denoising, restoration and feature extraction [1–4]. For example, discrete cosine transform (DCT) and discrete wavelet transform (DWT) are popularly used in image and video processing. DCT is adopted by JPEG, MPEG-2, and MPEG4/AVC, while DWT is adopted by JPEG2000 and used for digital cinema [1, 2]. These transforms, however, have a disadvantage in representing diagonal edges and textures due to the separability. From this background, development of image transforms involves non-separable construction for handling such diagonal structures [5–7]. The *oversampled* (OS) property is important as well as the non-separable property. Let us assume a P -channel filter bank. We denote the p th channel down- and upsampling factors as M_p . Then the sampling ratio of the p th channel, M_p , is given by $M_p = |\det(\mathbf{M}_p)|$. The total sum of the reciprocals of $\{M_p\}_{p=0}^{P-1}$, that is, $\sum_{p=0}^{P-1} \frac{1}{M_p}$ is called redundancy \mathcal{R} . When

$\mathcal{R} = 1$, the system is referred to as a *critically sampled* (CS) filter bank. The other case, $\mathcal{R} > 1$, is called an OS filter bank. Advantage of OS filter bank is its high degree of design freedom [5, 7–10]. There is infinite combination of analysis and synthesis banks in the OS case, while a CS system has unique combination.

Two simple ways are well known to construct OS filter banks from CS ones. One is a mixture construction of multiple CS systems, and the other is an undecimated, or shift-invariant construction, which is realized by removing the downsamplers and upsamplers from a CS system [10, 11]. The redundancy \mathcal{R} is, however, restricted to be integer in these approaches. In particular, the undecimated approach tends to have high redundancy. Undecimated Haar transform and Contourlets are known as OS systems. Undecimated Haar transform satisfies OS, linear-phase (LP) and paraunitary (PU) property, but does not have the non-separable property. On the other hand, Contourlets can satisfy the non-separable and OS property. However, simultaneous realization of the LP and PU property is restrictive due to the structure [9]. In general, the higher the redundancy is, the larger the computation and memory consumption become. From the fact, lower redundancy is requested while maintaining preferable properties for image processing. The authors have proposed two-dimensional (2D) non-separable oversampled lapped transforms (NSOLTs) as a new transform [12]. The transform is non-separable and can simultaneously satisfy the OS, compact-supported, LP, tight-frame, symmetric, real-valued, and overlapped property. NSOLTs are also equipped with no-DC-leakage option.

¹Graduate School of Science and Technology, Niigata University, Niigata 950-2181, Japan

²Canon Imaging Systems Inc., Niigata 950-0916, Japan

³Department of Electrical and Electronics Engineering, Niigata University, Niigata 950-2181, Japan

Corresponding author:

K. Furuya

Email: furuya@telecomeng.niigata-u.ac.jp

The redundancy can be controlled flexibly by the number of channels P and the sampling ratio M . NSOLTs with redundancy less than two were shown to be superior or comparable with the undecimated Haar wavelet transform in terms of image restoration performance [12, 13]. It is also possible to apply a learning-based dictionary design [14]. NSOLTs are verified to have comparable or superior sparse representation performance to Sparse K-SVD [15].

Managing the boundary is one of important issues in the image-processing applications, in order to reduce the boundary distortion. Note that the symmetric extension method is no longer applicable to NSOLTs unless the four-fold symmetry is imposed on every atom [16–18]. Although the periodic extension (PE) method can take the place of the symmetric extension method, it has drawbacks of wrapping effects and global memory access requirement at the border. We adopt a different approach for NSOLTs. In [19, 20], we have proposed a basis termination (BT) technique for non-separable CS lapped transforms, where the numbers of symmetric and anti-symmetric channels are restricted to be the same as each other. In this paper, we extend the BT technique for NSOLTs, i.e. the OS case, and propose a new technique which can deal with more general configuration. We refer to the proposed method as atom termination (AT) since NSOLTs are OS and the term “basis” is no longer appropriate.

The proposed technique is shown to serve variability of atoms block by block without any violation to the perfect reconstruction. It is also shown that a special selection of the lattice parameters breaks off an overlapping relation between neighboring blocks locally. By applying this property at the border, we can realize the AT.

This paper is an extended version of the conference paper [21]. The performance evaluation is revised to use the iterative hard thresholding (IHT) algorithm [22, 23] in order to decrease the influence of selection of a dual analysis dictionary. This paper is organized as follows: in Section II, as a preliminary, the lattice structure of 2D NSOLT is briefly reviewed. Section III derives the blockwise implementation technique for the lattice structure and the boundary operation with AT. Then, Section IV verifies the significance of the proposed method through experimental results with the IHT for some standard images, followed by conclusions in Section V.

II. REVIEW OF 2D NSOLT

NSOLT is a lattice structure realization of 2D non-separable oversampled linear-phase perfect reconstruction filter bank (NS-OSLPPRFB). Let us review the lattice structure of NSOLT.

First, we summarize some symbols and notations used throughout this paper. M_y and M_x are reserved for decimation factors in the vertical and horizontal directions, respectively. The total decimation factor is given by $M = M_y \times M_x$. As a preliminary, we define a $P \times P$ butterfly

matrix $\mathbf{B}_P^{(m)}$ as

$$\mathbf{B}_P^{(m)} = \begin{cases} \frac{1}{\sqrt{2}} \begin{pmatrix} \mathbf{I}_m & \mathbf{I}_m \\ \mathbf{I}_m & -\mathbf{I}_m \end{pmatrix}, & m = \frac{P}{2}, \\ \frac{1}{\sqrt{2}} \begin{pmatrix} \mathbf{I}_m & \mathbf{O} & \mathbf{I}_m \\ \mathbf{O} & \sqrt{2}\mathbf{I}_{P-2m} & \mathbf{O} \\ \mathbf{I}_m & \mathbf{O} & -\mathbf{I}_m \end{pmatrix}, & m < \frac{P}{2}, \end{cases} \quad (1)$$

where $\lceil M/2 \rceil \leq m \leq \lfloor P/2 \rfloor$, $\lceil \cdot \rceil$ and $\lfloor \cdot \rfloor$ are the ceiling function and the floor function, respectively.

Through out this paper, symbols \mathbf{O} and \mathbf{I}_m are reserved for the null and $m \times m$ identity matrix, respectively, where subscript m is omitted unless it is significant. A product of sequential matrices is denoted by $\prod_{n=1}^N \mathbf{A}_n = \mathbf{A}_N \mathbf{A}_{N-1} \mathbf{A}_{N-2} \cdots \mathbf{A}_2 \mathbf{A}_1$.

A) Lattice structure of 2D NSOLT

In the article [7], we showed a method to construct multidimensional non-separable linear-phase paraunitary filter banks (NS-LPPUFBs) with a lattice structure, and then, in [24], Gan and Ma showed the reduced parameterization. NSOLT is an extension of [7] to the OS case and can simultaneously hold the OS, compact-support, symmetric, real-valued, and overlapped property. It can also satisfy the PU property and realize a Parseval tight-frame. NSOLT is categorized into two types as:

- Type-I : $p_s = p_a$,
- Type-II : $p_s \neq p_a$,

where p_s and p_a denote the numbers of symmetric and antisymmetric atoms, respectively.

1) TYPE-I NSOLT

Figure 1(a) shows an example of Type-I NSOLT lattice structure. When the number of channels P is even, it is possible to set $p_s = p_a = P/2$. The polyphase matrix of Type-I NSOLT has the following product form:

$$\mathbf{E}(\mathbf{z}) = \prod_{n_y=1}^{N_y} \{\mathbf{R}_{n_y}^{(y)} \mathbf{Q}(z_y)\} \prod_{n_x=1}^{N_x} \{\mathbf{R}_{n_x}^{(x)} \mathbf{Q}(z_x)\} \mathbf{R}_0 \mathbf{E}_0, \quad (2)$$

where

$$\mathbf{Q}(z_d) = \mathbf{B}_P^{(P/2)} \begin{pmatrix} \mathbf{I}_{p_s} & \mathbf{O} \\ \mathbf{O} & z_d^{-1} \mathbf{I}_{p_a} \end{pmatrix} \mathbf{B}_P^{(P/2)},$$

$$\mathbf{R}_n^{(d)} = \begin{pmatrix} \mathbf{I}_{p_s} & \mathbf{O} \\ \mathbf{O} & \mathbf{U}_n^{(d)} \end{pmatrix},$$

where $\mathbf{U}_n^{(d)} \in \mathbb{R}^{p_a \times p_a}$ is an arbitrary non-singular matrix. We adopt the initial matrix defined by the product of the matrix representation of 2D DCT $\mathbf{E}_0 \in \mathbb{R}^{M \times M}$ and

$$\mathbf{R}_0 = \begin{pmatrix} \mathbf{W}_0 & \mathbf{O} \\ \mathbf{O} & \mathbf{U}_0 \end{pmatrix} \begin{pmatrix} \mathbf{I}_{\lceil M/2 \rceil} & \mathbf{O} \\ \mathbf{O} & \mathbf{O} \\ \mathbf{O} & \mathbf{I}_{\lfloor M/2 \rfloor} \\ \mathbf{O} & \mathbf{O} \end{pmatrix} \in \mathbb{R}^{P \times M}, \quad (3)$$

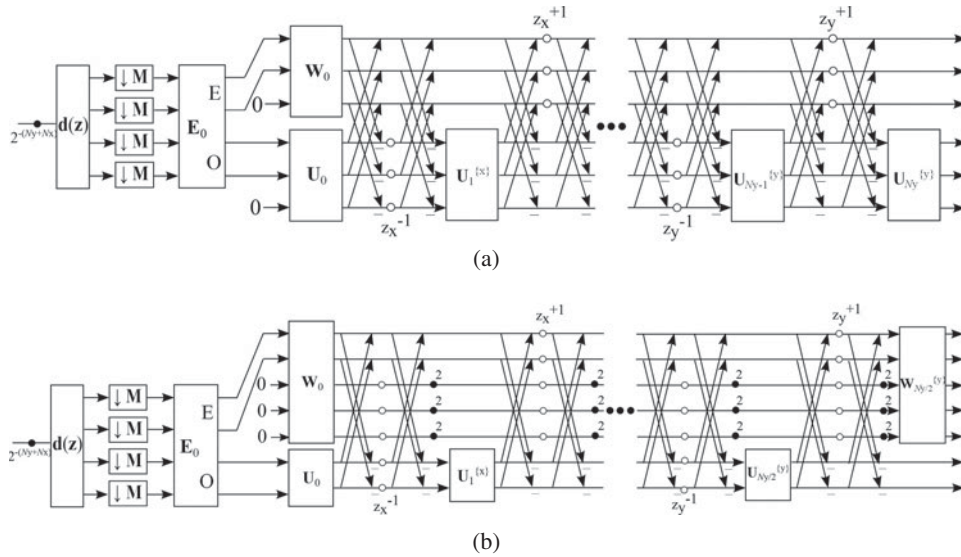


Fig. 1. Types I and II lattice structure of analysis NSOLT, where \mathbf{E}_0 denotes symmetric orthonormal transform matrix directly given by 2-D DCT, and $\mathbf{W}_0, \mathbf{U}_0, \mathbf{U}_n^{(d)}, \mathbf{U}_\ell^{(d)}$ and $\mathbf{W}_\ell^{(d)}$ are arbitrary invertible matrices. N_d is the order of the polyphase matrix in the direction $d \in \{y, x\}$, and $\mathbf{d}(\mathbf{z})$ is the delay chain determined by the downsampling factor $\mathbf{M} = \text{diag}(M_y, M_x)$. (a) Example of Type-I NSOLT. (#Channels $P = 6$, Sampling factor $M = 4$), (b) Example of Type II NSOLT. (#Channels $P = 7$, Sampling factor $M = 4, p_s > p_a$).

where $\mathbf{W}_0 \in \mathbb{R}^{p_s \times p_s}$ and $\mathbf{U}_0 \in \mathbb{R}^{p_a \times p_a}$ are arbitrary non-singular matrices. The matrices $\{\mathbf{R}_n^{(d)} \mathbf{Q}(z_d)\}$ realize the support extension of atoms, i.e., overlapping of atoms.

2) TYPE-II NSOLT

Figure 1(b) shows an example of Type-II NSOLT lattice structure. Type-II NSOLT is given when $p_s \neq p_a$. We here consider only the case $p_s > p_a$ with even N_y and even N_x . The polyphase matrix $\mathbf{E}(\mathbf{z})$ of Type-II is represented by the following product form:

$$\mathbf{E}(\mathbf{z}) = \prod_{\ell_y=1}^{N_y/2} \left\{ \mathbf{R}_{E\ell_y}^{(y)} \mathbf{Q}_E(z_y) \mathbf{R}_{O\ell_y}^{(y)} \mathbf{Q}_O(z_y) \right\} \times \prod_{\ell_x=1}^{N_x/2} \left\{ \mathbf{R}_{E\ell_x}^{(x)} \mathbf{Q}_E(z_x) \mathbf{R}_{O\ell_x}^{(x)} \mathbf{Q}_O(z_x) \right\} \mathbf{R}_0 \mathbf{E}_0, \quad (4)$$

where

$$\mathbf{Q}_E(z_d) = \mathbf{B}_P^{(p_a)} \begin{pmatrix} \mathbf{I}_{P-p_a} & \mathbf{O} \\ \mathbf{O} & z_d^{-1} \mathbf{I}_{p_a} \end{pmatrix} \mathbf{B}_P^{(p_a)},$$

$$\mathbf{Q}_O(z_d) = \mathbf{B}_P^{(p_a)} \begin{pmatrix} \mathbf{I}_{p_a} & \mathbf{O} \\ \mathbf{O} & z_d^{-1} \mathbf{I}_{P-p_a} \end{pmatrix} \mathbf{B}_P^{(p_a)},$$

$$\mathbf{R}_{E\ell}^{(d)} = \begin{pmatrix} \mathbf{W}_\ell^{(d)} & \mathbf{O} \\ \mathbf{O} & \mathbf{I}_{p_a} \end{pmatrix}, \quad \mathbf{R}_{O\ell}^{(d)} = \begin{pmatrix} \mathbf{I}_{p_s} & \mathbf{O} \\ \mathbf{O} & \mathbf{U}_\ell^{(d)} \end{pmatrix}.$$

$\mathbf{W}_\ell^{(d)} \in \mathbb{R}^{p_s \times p_s}$ and $\mathbf{U}_\ell^{(d)} \in \mathbb{R}^{p_a \times p_a}$ are arbitrary invertible matrices. We adopt the initial matrix defined by the product of the 2D DCT $\mathbf{E}_0 \in \mathbb{R}^{M \times M}$ and $\mathbf{R}_0 \in \mathbb{R}^{P \times M}$ in (3). The matrices $\{\mathbf{R}_{E\ell}^{(d)} \mathbf{Q}_{E\ell}^{(d)} \mathbf{R}_{O\ell}^{(d)} \mathbf{Q}_{O\ell}^{(d)}\}$ realize the support extension of atoms.

B) Lattice structure with advance shifters

In the spatial domain, advance shifters are allowed as well as delay shifters. For the later discussion, we consider modifying $\mathbf{Q}(z_d)$ and $\mathbf{Q}_E(z_d)$ in each type of NSOLT by introducing the advance shifters.

1) TYPE-I NSOLT

Let us define

$$\bar{\mathbf{Q}}(z_d) = z_d \mathbf{Q}(z_d) = \mathbf{B}_P^{(P/2)} \begin{pmatrix} z_d \mathbf{I}_{p_s} & \mathbf{O} \\ \mathbf{O} & \mathbf{I}_{p_a} \end{pmatrix} \mathbf{B}_P^{(P/2)}.$$

Then, we can rewrite (2) for even N_y and N_x as

$$\mathbf{E}(\mathbf{z}) = z_y^{-\frac{N_y}{2}} z_x^{-\frac{N_x}{2}} \prod_{n_y=1}^{N_y/2} \left\{ \mathbf{R}_{2n_y}^{(y)} \bar{\mathbf{Q}}(z_y) \mathbf{R}_{2n_y-1}^{(y)} \mathbf{Q}(z_y) \right\} \times \prod_{n_x=1}^{N_x/2} \left\{ \mathbf{R}_{2n_x}^{(x)} \bar{\mathbf{Q}}(z_x) \mathbf{R}_{2n_x-1}^{(x)} \mathbf{Q}(z_x) \right\} \mathbf{R}_0 \mathbf{E}_0. \quad (5)$$

Figure 1(a) shows the lattice structure which corresponds to (5), where we omit to illustrate delays $z_y^{-N_y/2}$ and $z_x^{-N_x/2}$ since they are less significant later. Note that the operation with $\mathbf{Q}(z_d)$ is realized by the combination of the following matrices:

$$\mathbf{B}_P^{(P/2)} = \frac{1}{\sqrt{2}} \begin{pmatrix} \mathbf{I}_{P/2} & \mathbf{I}_{P/2} \\ \mathbf{I}_{P/2} & -\mathbf{I}_{P/2} \end{pmatrix},$$

$$\mathbf{A}(z_d) = \begin{pmatrix} \mathbf{I}_{p_s} & \mathbf{O} \\ \mathbf{O} & z_d^{-1} \mathbf{I}_{p_a} \end{pmatrix}$$

as $\mathbf{Q}(z_d) = \mathbf{B}_P^{(P/2)} \mathbf{\Lambda}(z_d) \mathbf{B}_P^{(P/2)}$. Then, the operation with $\overline{\mathbf{Q}}(z_d)$ is realized by $\mathbf{B}_P^{(P/2)}$ and

$$\overline{\mathbf{\Lambda}}(z_d) = \begin{pmatrix} z_d \mathbf{I}_{p_s} & \mathbf{O} \\ \mathbf{O} & \mathbf{I}_{p_a} \end{pmatrix}$$

as $\overline{\mathbf{Q}}(z_d) = \mathbf{B}_P^{(P/2)} \overline{\mathbf{\Lambda}}(z_d) \mathbf{B}_P^{(P/2)}$.

2) TYPE-II NSOLT WITH $p_s > p_a$

Similarly, using the advance shifters, Type-II NSOLT is realized by

$$\overline{\mathbf{Q}}_E(z_d) = z_d \mathbf{Q}_E(z_d) = \mathbf{B}_P^{(p_a)} \begin{pmatrix} z_d \mathbf{I}_{P-p_a} & \mathbf{O} \\ \mathbf{O} & \mathbf{I}_{p_a} \end{pmatrix} \mathbf{B}_P^{(p_a)}.$$

Then, we can rewrite (4) for even N_y and N_x as

$$\mathbf{E}(\mathbf{z}) = z_y^{-\frac{N_y}{2}} z_x^{-\frac{N_x}{2}} \prod_{\ell_y=1}^{N_y/2} \left\{ \mathbf{R}_{E\ell_y}^{[y]} \overline{\mathbf{Q}}_E(z_y) \mathbf{R}_{O\ell_y}^{[y]} \mathbf{Q}_O(z_y) \right\} \times \prod_{\ell_x=1}^{N_x/2} \left\{ \mathbf{R}_{E\ell_x}^{[x]} \overline{\mathbf{Q}}_E(z_x) \mathbf{R}_{O\ell_x}^{[x]} \mathbf{Q}_O(z_x) \right\} \mathbf{R}_0 \mathbf{E}_0. \quad (6)$$

Figure 1(b) illustrates the lattice structure for (6), where we omit to draw the delays $z_y^{-N_y/2}$ and $z_x^{-N_x/2}$. Here, note that $\mathbf{Q}_E(z_d)$ is realized by the combination of the following matrices:

$$\mathbf{B}_P^{(p_a)} = \frac{1}{\sqrt{2}} \begin{pmatrix} \mathbf{I}_{p_a} & \mathbf{O} & \mathbf{I}_{p_a} \\ \mathbf{O} & \sqrt{2} \mathbf{I}_{P-2p_a} & \mathbf{O} \\ \mathbf{I}_{p_a} & \mathbf{O} & -\mathbf{I}_{p_a} \end{pmatrix},$$

$$\mathbf{\Lambda}(z_d) = \begin{pmatrix} \mathbf{I}_{P-p_a} & \mathbf{O} \\ \mathbf{O} & z_d^{-1} \mathbf{I}_{p_a} \end{pmatrix}$$

as $\mathbf{Q}_E(z_d) = \mathbf{B}_P^{(p_a)} \mathbf{\Lambda}(z_d) \mathbf{B}_P^{(p_a)}$. In addition, $\overline{\mathbf{Q}}_E(z_d)$ is realized by $\mathbf{B}_P^{(p_a)}$ and

$$\overline{\mathbf{\Lambda}}(z_d) = \begin{pmatrix} z_d \mathbf{I}_{P-p_a} & \mathbf{O} \\ \mathbf{O} & \mathbf{I}_{p_a} \end{pmatrix},$$

that is, $\overline{\mathbf{Q}}_E(z_d) = \frac{1}{2} \mathbf{B}_P^{(p_a)} \overline{\mathbf{\Lambda}}(z_d) \mathbf{B}_P^{(p_a)}$.

III. BOUNDARY OPERATION

In this section, we illustrate blockwise implementation of NSOLT based on the lattice structure, and propose the boundary operation for AT. Note that we describe them for Type-II NSOLT mainly because the way of the primitive block operations and the boundary operation for Type-II NSOLT are different from the previous work in [19]. Thus, this is the main contribution of this work. In contrast, these operations for Type-I NSOLT are almost the same as [19] so that we omit to show the details of primitive block operations and the boundary operation for Type-I NSOLT.

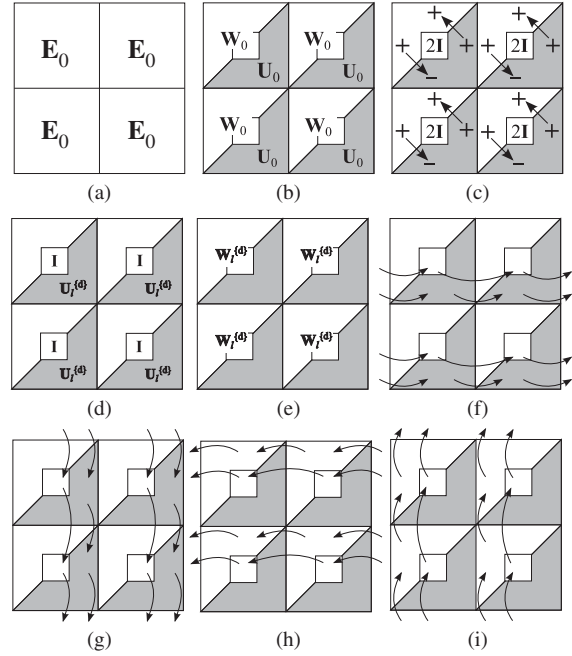


Fig. 2. Primitive block operations for Type-II NSOLT, where the white and shaded regions mean operations for upper and lower half intermediate coefficient vectors, respectively, where \mathbf{I} in the center block is the identity matrix for center intermediate coefficient. (a) \mathbf{E}_0 , (b) \mathbf{R}_0 , (c) $\mathbf{B}_P^{(p_a)}$, (d) $\mathbf{R}_{O\ell}^{[d]}$, (e) $\mathbf{R}_{E\ell}^{[d]}$, (f) $\mathbf{\Lambda}(z_x)$, (g) $\mathbf{\Lambda}(z_y)$, (h) $\overline{\mathbf{\Lambda}}(z_x)$, and (i) $\overline{\mathbf{\Lambda}}(z_y)$.

A) Primitive block operations

1) TYPE-I NSOLT

The primitive block operation for Type-I NSOLT is realized using the operations in Fig. 2. These operations are detailed in next paragraph section. Note that the center block vanishes from the block operations for Type-I NSOLT.

2) TYPE-II NSOLT WITH $p_s > p_a$

Figure 2 summarizes the primitive block operations required for analyzing an image based on the product form of (6), where 2×2 neighboring blocks are illustrated. Combination of these primitive operations can implement the analysis process, as in Fig. 1(b). Because the synthesis process is realized through the inverse primitive operations in reverse order, we omit to show the detail.

The first operation with delay chain $\mathbf{d}(\mathbf{z})$, downsampling by factor $\mathbf{M}(= \text{diag}(M_y, M_x))$, and the transform by matrix \mathbf{E}_0 in Fig. 1 are exactly the same as the 2D block DCT, which is shown in Fig. 2(a). Note that operation (a) is adopted to the block before inserting the center block coefficient. After dividing the 2D DCT coefficients into two sets according to the atom symmetry, that is, even or odd symmetry, the transform with matrix \mathbf{R}_0 is applied as in Fig. 2(b), where the white and shaded regions except the center block show operations for intermediate coefficients analyzed by the even- and odd-symmetric 2D DCT basis images.

Figures 2(c)–(i) relate to the support extension of atoms. Figure 2(c) shows the operation with $\mathbf{B}_P^{(p_a)}$. This is nothing but the butterfly calculation. Figure 2(d) illustrates the transform corresponds to matrix $\mathbf{R}_{O\ell}^{[d]}$ that processes only

the lower half intermediate coefficients through matrix $U_\ell^{(d)}$. In Fig. 2(e), the matrix $R_{E\ell}^{(d)}$ is applied to the upper half intermediate coefficients including the center block through matrix $W_\ell^{(d)}$. Operations $\Lambda(z_x)$ and $\Lambda(z_y)$ in Figs 2(f) and (g) delay the lower half intermediate coefficients. $\Lambda(z_x)$ borrows the coefficients from the left block. Similarly, $\Lambda(z_y)$ shifts the left block coefficients from the upper block. Figures 2(h) and (i) illustrate the operations of $\bar{\Lambda}(z_x)$ and $\bar{\Lambda}(z_y)$, which return the upper half coefficients to the left and upper blocks, respectively. These primitive block operations are applied to every block in the order indicated by (6).

Note that all of the operations illustrated in Figs 2(a)–(e) are independent of the other blocks. Although the delay and advance shift operations shown in Figs 2(f)–(i) depend on the others, the relation is limited to the neighboring blocks. Therefore, the non-singular matrices $W_0, U_0, U_\ell^{(d)}$, and $W_\ell^{(d)}$ can vary block by block without any violation to the perfect reconstruction of the whole system.

B) Boundary operation

The boundary treatment should be taken into account for some image analysis–synthesis systems since it can cause distortion at boundary for the image processing applications. Unfortunately, the popular symmetric extension approach is not available for NSOLT unless the fourfold symmetry is satisfied.

As a solution, we propose to terminate the dependence between neighboring blocks by shrinking the support region of atoms. In Type-I NSOLT, AT can be realized by locally making the support extension stages $\{R_{2n_d} \bar{Q}(z_d) R_{2n_d-1} Q(z_d)\}$ null order, i.e., independent of z_d . This purpose is achieved if we can cancel the delay and advance shifters out locally and make the support extension invalid. In Type-II NSOLT, it can be realized by making $\{R_{E\ell}^{(d)} \bar{Q}_E(z_d) R_{O\ell}^{(d)} Q_O(z_d)\}$ null order local. Let us show how to realize the AT process in each type of NSOLT.

1) TYPE-I NSOLT

AT for Type-I NSOLT can be realized by locally setting $U_{2n-1}^{(d)} = -I$ as follows:

$$\begin{aligned} & \bar{Q}(z_d) R_{2n-1}^{(d)} Q(z_d) \\ &= B_P^{(P/2)} \begin{pmatrix} z_d I_{p_s} & \mathbf{O} \\ \mathbf{O} & I_{p_a} \end{pmatrix} B_P^{(P/2)} \\ & \quad \times \begin{pmatrix} \mathbf{I} & \mathbf{O} \\ \mathbf{O} & U_n^{(d)} \end{pmatrix} B_P^{(P/2)} \begin{pmatrix} I_{p_s} & \mathbf{O} \\ \mathbf{O} & z_d^{-1} I_{p_a} \end{pmatrix} B_P^{(P/2)} \\ &= \frac{1}{4} \begin{pmatrix} (z_d + 1)I & (z_d - 1)I \\ (z_d - 1)I & (z_d + 1)I \end{pmatrix} \\ & \quad \times \begin{pmatrix} \mathbf{I} & \mathbf{O} \\ \mathbf{O} & -I \end{pmatrix} \begin{pmatrix} (1 + z_d^{-1})I & (1 - z_d^{-1})I \\ (1 - z_d^{-1})I & (1 + z_d^{-1})I \end{pmatrix} \\ &= \frac{1}{4} \begin{pmatrix} (z_d + 1)I & (1 - z_d)I \\ (z_d - 1)I & -(z_d + 1)I \end{pmatrix} \end{aligned}$$

$$\begin{aligned} & \times \begin{pmatrix} (1 + z_d^{-1})I & (1 - z_d^{-1})I \\ (1 - z_d^{-1})I & (1 + z_d^{-1})I \end{pmatrix} \\ &= \begin{pmatrix} \mathbf{I} & \mathbf{O} \\ \mathbf{O} & -I \end{pmatrix}, \end{aligned} \tag{7}$$

where

$$\begin{aligned} B_P^{(P/2)} &= \frac{1}{\sqrt{2}} \begin{pmatrix} \mathbf{I} & \mathbf{I} \\ \mathbf{I} & -\mathbf{I} \end{pmatrix}, \\ R_n^{(d)} &= \begin{pmatrix} I_{p_s} & \mathbf{O} \\ \mathbf{O} & U_n^{(d)} \end{pmatrix}. \end{aligned}$$

Equation (7) shows that the Type-I NSOLT can cancel the overlapping property of atoms. If the horizontal parameter matrices $U_{2n-1}^{(x)}$ for all n in a block set to $-I$, the relation of the current block to the left block is terminated. In addition, the vertical parameter matrices $U_{2n-1}^{(y)}$ for all n in a block to $-I$ terminates the relation of the current block to the upper block. This relation is equivalent to the BT in [19] because the number of upper and lower half intermediate coefficients are $p_s = p_a = \frac{P}{2}$. From this fact, for Type-I NSOLT, the AT procedure becomes almost the same as the BT procedure. Thus, we omit to show the detailed derivation of AT for Type-I NSOLT.

AT for Type-II NSOLT is, however, different from the Type-I case. The difference appears in the implementation of Figs 4(c) and (g) for coefficient shift processes. In the case of Type-I NSOLT, these processes are applied to only upper and lower half intermediate coefficients except for the center block.

2) TYPE-II NSOLT

Type-II NSOLT AT can be realized by locally setting for $U_\ell^{(d)} = -I$ as follows:

$$\begin{aligned} & \bar{Q}_E(z_d) R_{O\ell}^{(d)} Q_O(z_d) \\ &= B_P^{(p_a)} \begin{pmatrix} z_d I_{P-p_a} & \mathbf{O} \\ \mathbf{O} & I_{p_a} \end{pmatrix} B_P^{(p_a)} \times \begin{pmatrix} I_{p_a} & \mathbf{O} \\ \mathbf{O} & U_\ell^{(d)} \end{pmatrix} \\ & B_P^{(p_a)} \begin{pmatrix} I_{p_a} & \mathbf{O} \\ \mathbf{O} & z_d^{-1} I_{P-p_a} \end{pmatrix} B_P^{(p_a)} \\ &= \frac{1}{4} \begin{pmatrix} (z_d + 1)I_{p_a} & \mathbf{O} & (1 - z_d)I_{p_a} \\ \mathbf{O} & 2z_d I_{P-p_a} & \mathbf{O} \\ (z_d - 1)I_{p_a} & \mathbf{O} & -(z_d + 1)I_{p_a} \end{pmatrix} \\ & \quad \times \begin{pmatrix} (1 + z_d^{-1})I_{p_a} & \mathbf{O} & (1 - z_d^{-1})I_{p_a} \\ \mathbf{O} & 2z_d I_{P-p_a} & \mathbf{O} \\ (1 - z_d^{-1})I_{p_a} & \mathbf{O} & (1 + z_d^{-1})I_{p_a} \end{pmatrix} \\ &= \begin{pmatrix} I_{P-p_a} & \mathbf{O} \\ \mathbf{O} & -I_{p_a} \end{pmatrix}, \end{aligned} \tag{8}$$

where

$$\begin{aligned} B_P^{(p_a)} &= \frac{1}{\sqrt{2}} \begin{pmatrix} I_{p_a} & \mathbf{O} & I_{p_a} \\ \mathbf{O} & \sqrt{2} I_{P-2m} & \mathbf{O} \\ I_{p_a} & \mathbf{O} & -I_{p_a} \end{pmatrix}, \\ R_{O\ell}^{(d)} &= \begin{pmatrix} I_{p_a} & \mathbf{O} \\ \mathbf{O} & U_\ell^{(d)} \end{pmatrix}. \end{aligned}$$

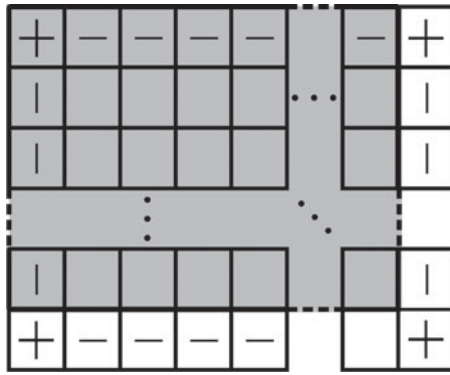


Fig. 3. Boundary operation with AT, where the shaded area denotes the original support region of a given image. The blocks including ‘0’, ‘-’ and ‘+’ denote termination blocks in the horizontal, vertical, and both directions, respectively.

From (8), Type-II NSOLT can also control the overlapping property of atoms. It is noticed that the relation in (8) reduces the number of overlapping blocks in direction $d \in \{y, x\}$. If the horizontal parameter matrices $U_\ell^{(x)}$ for all ℓ in a block set to $-\mathbf{I}$, the relation of the current block to the left block is terminated. In addition, the vertical parameter matrices $U_\ell^{(y)}$ for all ℓ in a block to $-\mathbf{I}$ terminates the relation of the current block to the upper block.

Figure 3 illustrates the termination block position, where the blocks including ‘0’, ‘-’ and ‘+’ denote the termination blocks in the horizontal, vertical, and both directions. Around the original picture, any value can be assumed

since they have no influence on the essential transform coefficients.

Figure 4 illustrates the local AT procedure in the blockwise operation for Type-II NSOLT, where succeeding three blocks are denoted. Note that the discussion holds for both the horizontal and vertical directions. In Fig. 4(a), u_b and v_b denote upper and lower intermediate coefficients, where b means the relative position from the current block. As well, the c_b in the center block contains a part of upper half intermediate coefficients vector. The next step is the butterfly operation with $B_p^{(p_a)}$ for u_b and v_b block by block in Fig. 4(b), where $w_b = u_b + v_b$ and $x_b = u_b - v_b$. The butterfly operations are not adopted to c_b . Then, each lower vector x_b and the center block c_b are moved to next block as shown in Fig. 4(c). After the operation Fig. 4(c), the butterfly operation is applied to vectors u_b and v_b again as in Fig. 4(d). In Fig. 4(e), the transform with $U_\ell^{(d)}$ is applied to each lower vector, where we set $U_\ell^{(d)} = -\mathbf{I}$ for the block of interest in the thick frame. After the butterfly operation in Fig. 4(f), each upper vector is advanced to the previous block, as shown in Fig. 4(g), and the butterfly operation is applied to as in Fig 4(h).

Note that the left block of the vertical dashed line in Fig. 4(h) is independent of the coefficients for $b \geq 0$. Similarly, the right block is independent of the coefficients for $b < 0$. These facts imply that these blocks have no relation to each other. That is, the atoms are terminated at the vertical dashed line without any violation to the perfect reconstruction.

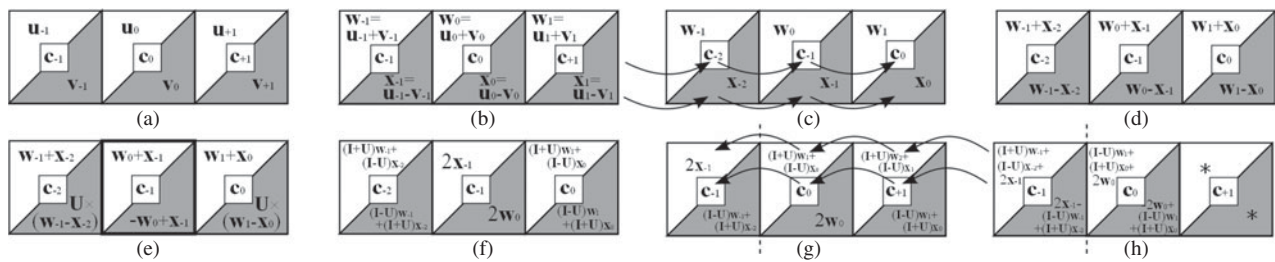


Fig. 4. AT flow of the blockwise operations corresponding to (8), where succeeding three blocks are exemplified. (a) Intermediate coefficients of each blocks. (b) Operation with $B_p^{(m)}$. (c) Operation with $\Lambda(z_x)$. (d) Operation with $B_p^{(p_a)}$. (e) Operation with $R_{O_\ell}^{(d)}$. (f) Operation with $B_p^{(m)}$. (g) Operation with $\bar{\Lambda}(z_x)$. (h) Operation with $B_p^{(m)}$. These operations from (a) to (h) are applied alphabetical order, where $U = U_\ell^{(d)}$. In (e), the thick frame shows that the block to which parameter $U_\ell^{(d)} = -\mathbf{I}$ is applied. The vertical dashed line in (g) and (h) denotes the separation of dependence between the blocks. For convenience, we omit to show the details in the right block in (h). Note that c_b in center block is operation of inserting zero in Fig. 1.

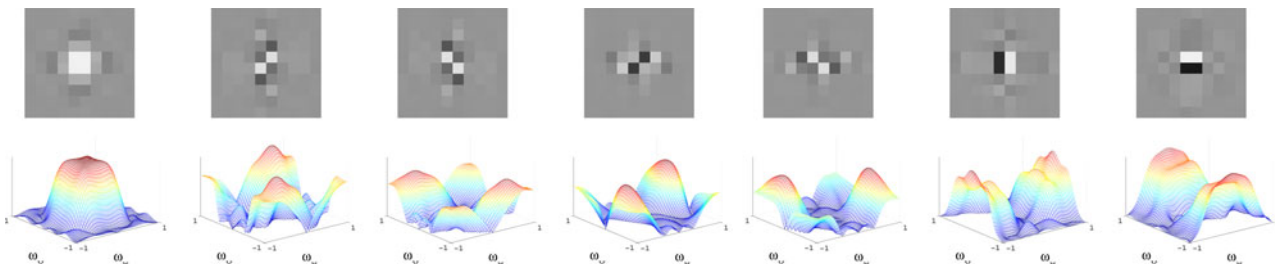


Fig. 5. Design example of Type-II NSOLT, where the impulse responses are shown in the top, and frequency amplitude responses are shown in the bottom, where $P = p_a + p_s = 7$, $M_y = M_x = 2(M = 4)$, and $N_y = N_x = 4$.

IV. EXPERIMENTAL RESULT

Let us verify the significance of the proposed AT technique. Different from [21], the IHT algorithm was adopted in this experiment. In this experiment, we use filters of three different extent, where polyphase order (N_y, N_x) are set to $(2, 2)$, $(4, 4)$ and $(6, 6)$. Figure 5 shows an example set

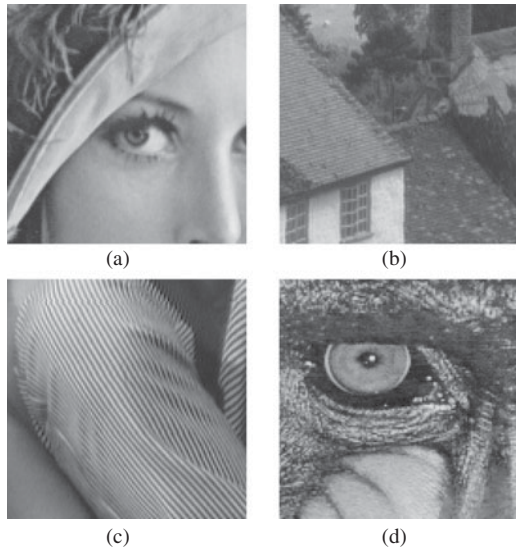


Fig. 6. Original images of size 128×128 , 8-bit grayscale. (a) *lena*, (b) *goldhill*, (c) *barbara*, and (d) *baboon*.

Table 1. Experimental settings of IHT with NSOLT.

Downsampl. M	2×2
#Channels P	7
Polyphase order	$(2, 2)$, $(4, 4)$, $(6, 6)$
#Transform Coefs.	500

of impulse responses and frequency amplitude responses designed using the method in [12]. Figure 6 shows original images in this experiment. We apply each image to NSOLT with PE and AT. Parameter setting of NSOLT is shown in Table 1. Figure 7 shows eight examples of the terminated atom sets and one normal atom set. It is observed that the region of support is properly controlled through the local termination process. These atoms are no longer symmetric at the border. However, they keep the PR property and prevent the wrapping effect caused by the PE method.

Figure 8 shows a part of experimental results of IHT with NSOLT of polyphase $(N_y, N_x) = (4, 4)$. The original picture is given in Figs 8(a)–(c) show the reconstruction results of PE and AT, respectively. From Fig. 8, it is observed that the PE method occurs wrapping effect at the right and bottom boundary, while the AT method, does not. Table 2 shows peak signal-to-noise ratio (PSNR) for NSOLT of different polyphase order. From Table 2, NSOLT with AT gives a higher PSNR than that with PE in each case.

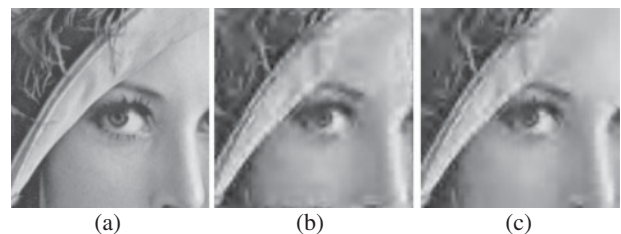


Fig. 8. A part of experimental result with IHT in the case of $(N_y, N_x) = (4, 4)$. (a) Original. (b) NSOLT with PE (PSNR: 26.80 [dB]). (c) NSOLT with AT (PSNR: 28.12 [dB]). In this experiment, six-level hierarchical 2D wavelet construction was adopted and the number of transform coefficients in IHT was set to 500.

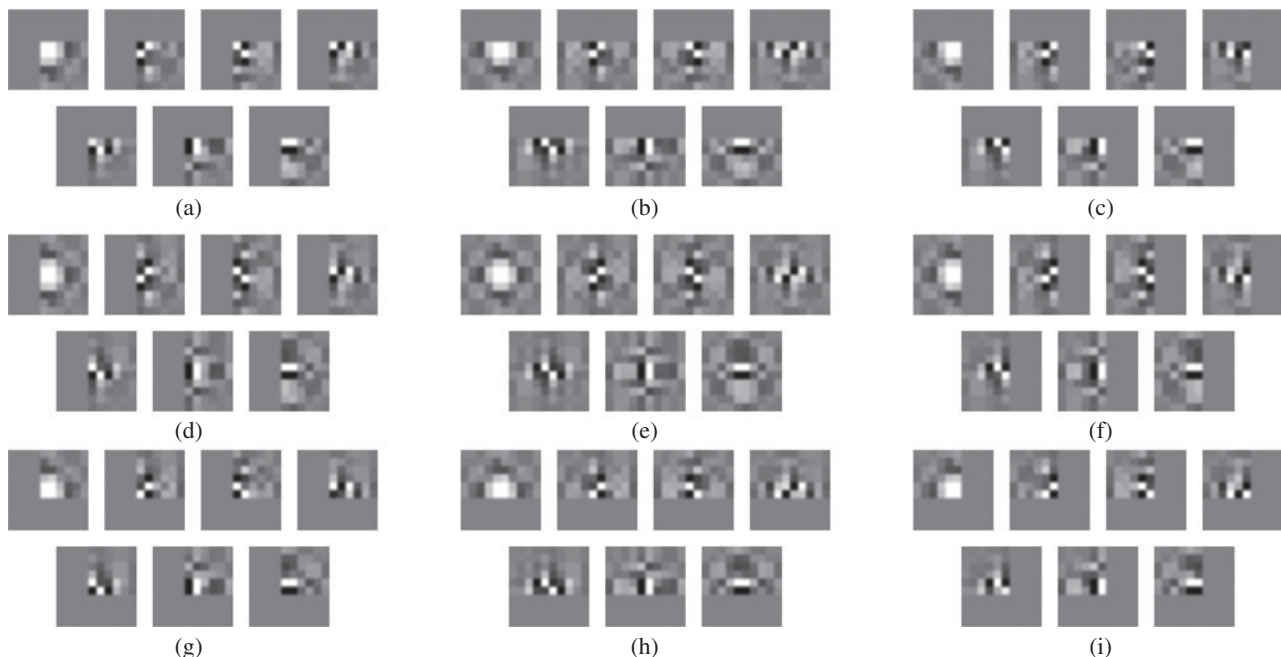


Fig. 7. Examples of terminated atom sets and the original normal atom set, where the contrast of each atom is enhanced in order to clarify the region of support. (a) Top left. (b) Top. (c) Top right. (d) Left. (e) Normal. (f) Right. (g) Bottom left. (h) Bottom. (i) Bottom right.

Table 2. Experimental result of PSNR (dB) with PE and AT.

Polyphase order	Images	PE	AT
(2, 2)	Lena	26.26	27.20
	Goldhill	27.29	27.52
	Barbara	21.50	21.74
	Baboon	21.01	21.14
(4, 4)	Lena	26.80	28.12
	Goldhill	27.31	27.80
	Barbara	21.71	22.02
	Baboon	21.17	21.32
(6, 6)	Lena	26.63	28.35
	Goldhill	27.26	27.90
	Barbara	21.77	22.10
	Baboon	21.25	21.53

V. CONCLUSION

In this work, we proposed a blockwise implementation of 2D NSOLTs and a boundary operation technique. This technique was shown to serve local variability of atoms without any violation of the perfect reconstruction. The blockwise implementation is effective for the image processing application since it allows us to control the region of support locally and leads an AT to prevent distortion at image boundary. Through experiments with IHT, we verified the significance of the proposed AT.

ACKNOWLEDGEMENT

This work was supported by KAKENHI (Grant no. 26420347).

REFERENCES

- [1] Rao, K.R.; Yip, P.C. eds.: *The Transform and Data Compression Handbook*, Crc Pr I Llc, 2000.
- [2] Taubman, D.S.; Marcellin, M.W.: *JPEG2000, Image Compression Fundamentals, Standards and Practic*, *Kluwer Academic Publishers*, Massachusetts, 2002.
- [3] Vaidynathan, P.P.: *Multirate Systems and Filter Banks*, *Prentice-Hall*, New Jersey, 1993.
- [4] Vetterli, M.; Kovačević, J.: *Wavelets and Subband Coding*, *Prentice-Hall*, New Jersey, 1995.
- [5] Vetterli, M.: Wavelets, approximation, and compression. *IEEE Signal Process. Mag.*, **18**, (5) (2001), 59–73.
- [6] Mallat, S.: A Wavelet tour of signal processing, in *The Sparse Way*, 3rd ed., *Academic*, New York, 2008.
- [7] Muramatsu, S.; Yamada, A.; Kiya, H.: A design method of multidimensional linear-phase paraunitary filter banks with a lattice structure. *IEEE Trans. Signal Proc.*, **47** (3) (1999), 690–700.
- [8] Kovačević, J.; Chebira, A.: Life beyond bases: the advent of frames (Part I). *IEEE Signal Process. Mag.*, **24** (4) (2007), 86–104.
- [9] Do, M.N.; Vetterli, M.: The contourlet transform: An efficient directional multiresolution image representation. *IEEE Trans. Image Process.*, **14** (12) (2005), 2091–2106.
- [10] Starck, J.-L.; Murtagh, F.; Fadili, J.M.: *Sparse Image and Signal Processing: Wavelets, Curvelets, Morphological Diversity*. *Cambridge University Press*, Cambridge, UK, 2010.
- [11] Muramatsu, S.; Han, D.; Kobayashi, T.; Kikuchi, H.: Directional lapped orthogonal transform: theory and design. *IEEE Trans. Image Process.*, **21** (5) (2012), 2434–2448.
- [12] Muramatsu, S.; Aizawa, N.: Lattice structure for 2-D Non-separable oversampled lapped transforms, in *Proc. IEEE ICASSP*, Vancouver, Canada, May 2013, 5632–5636.
- [13] Muramatsu, S.; Aizawa, N.: Image restoration with 2-D non-separable oversampled lapped transforms, in *Proc. IEEE ICIP*, Melbourne, Australia, September 2013, 1051–1055.
- [14] Muramatsu, S.: Structured dictionary learning with 2-D non-separable oversampled lapped transforms, in *Proc. of IEEE ICASSP*, Florence, Italy, May 2014, 2643–2647.
- [15] Rubinstein, R.; Zibulevsky, M.; Elad, M.: Double sparsity: Learning sparse dictionaries for sparse signal approximation. *IEEE Trans. Signal Process.*, **46** (3) (2010), 1553–1564.
- [16] Kiya, H.; Nishikawa, K.; Iwahashi, M.: A development of symmetric extension method for subband image coding. *IEEE Trans. Image Process.*, **3** (1) (1994), 78–81.
- [17] Chen, L.; Nguyen, T.Q.; Chan, K.-P.: Symmetric extension methods for M-channel linear-phase perfect-reconstruction filter banks. *IEEE Trans. Signal Process.*, **43** (11) (1995), 2505–2511.
- [18] Muramatsu, S.; Yamada, A.; Kiya, H.: The two-dimensional lapped Hadamard transform. *IEICE Trans. Fundam.*, **E81-A** (8) (1998), 1542–1549.
- [19] Muramatsu, S.; Kobayashi, T.; Hiki, M.; Kikuchi, H.: Boundary operation of 2-D non-separable linear-phase paraunitary filter banks. *IEEE Trans. Image Process.*, **21** (4) (2012), 2314–2318.
- [20] Muramatsu, S.; Hiki, M.: Block-wise implementation of directional GenLOT, in *Proc. IEEE ICIP*, Cairo, Egypt, November 2009, 3977–3980.
- [21] Furuya, K.; Hara, S.; Muramatsu, S.: Boundary operation of 2-D non-separable oversampled lapped transforms, in *Proc. of APSIPA ASC*, Kaohsiung, Taiwan, November 2013.
- [22] Blumensath, T.; Davies, M.E.: Iterative hard thresholding for compressed sensing. *Appl. Comput. Harmon. Anal.*, **27** (3) (2009), 265–274.
- [23] Blumensath, T.; Davies, M.E.: Normalized iterative hard thresholding: Guaranteed stability and performance. *IEEE J. sel. Topics Signal Process.*, **4** (2) (2010), 298–309.
- [24] Gan, L.; Ma, K.-K.: A simplified lattice factorization for linear-phase perfect reconstruction filter bank. *IEEE Signal Process. Lett.*, **8** (7) (2001), 207–209.

Kosuke Furuya received his B.E. degree in Electrical and Electronic Engineering from Niigata University, Japan, in 2013. He received the M.E. degree in Electrical and Information Engineering from Graduate School of Niigata University and he joined Toyota Motor Corp. in 2015. His research interests include image processing.

Shintaro Hara received the B.E. degree in Electrical and Electronic Engineering from Niigata University in 2012. He received the M.E. degree in Electrical and Information Engineering from Graduate School of Science and Technology, Niigata University, and he joined Canon Imaging Systems Inc. in 2014.

Kenta Seino received B.E. degree in Electrical and Electronic Engineering from Niigata University in 2014. He is currently registered at graduate school of Niigata University. His research interests are in image processing. He received the Electrical Academic Incentive Award from the Institute of Electrical Engineers of Japan in 2014.

Shogo Muramatsu received B.E., M.E., and Ph.D. degrees from Tokyo Metropolitan University in 1993, 1995, and 1998, respectively. From 1997 to 1999, he worked at Tokyo Metropolitan University. In 1999, he joined Niigata University, where

he is currently an Associate Professor in the Department of Electrical and Electronics Engineering, Faculty of Engineering. During year from 2003 to 2004, he was a visiting researcher at the University of Florence, Italy. His research interests are in multidimensional signal processing, multirate systems, image processing, video analysis, and embedded vision systems. Dr. Muramatsu is a senior member of IEEE (The Institute of Electrical and Electronics Engineers, Inc.) and IEICE (Institute of Electronics, Information and Communication Engineers of Japan), and a member of ITE (Institute of Image Information and Television Engineers of Japan).